JOURNAL OF ENERGY, MATERIALS, AND INSTRUMENTATION TECHNOLOGY

Journal Webpage https://jemit.fmipa.unila.ac.id/

The Effect of Chitosan Addition on Phase Composition and Detection Sensitivity of Fe_3O_4/Chitosan Magnetic Label Nanoparticles Based on Giant Magnetoresistance Sensor

Galih Aji Prayoga, Yuvita Oktarisa*, Ganesha Antarnusa*, Nur Shabrina Fitriani, Refi Meilia Aryani, Andri Suherman, and Yudi Guntara

Department of Physics Education, Faculty of Teacher Training and Education, Universitas Sultan Ageng Tirtayasa, Serang, Indonesia

Article Information

Article history:
Received Ocotber 13, 2024
Received in revised form November 5, 2024
Accepted November 7, 2024

Keywords: *Giant Magnetoresistance, Fe_3O_4/chitosan, Magnetic label, co-precipitation, Sensor*

Abstract

This study describes how phase composition affects the ability of giant magnetoresistance (GMR) chip-based sensors to detect magnetic labels made of Fe_3O_4 and Fe_3O_4/chitosan that were synthesized using the co-precipitation method. X-ray diffraction (XRD) analysis revealed that the synthesized nanoparticles were a mixture of magnetite and maghemite phases. The most intense diffraction peak at 2θ = 35.6° (311) confirmed the presence of the magnetite phase. The addition of chitosan significantly increased the proportion of the maghemite phase from 10% to 25%, with the appearance of an additional peak at 2θ = 33° (221). The modification of Fe_3O_4 nanoparticles into Fe_3O_4/chitosan nanocomposites resulted in changes in sensor sensitivity. The GMR sensor successfully detected Fe_3O_4 and Fe_3O_4/chitosan magnetic labels within 30 seconds with high sensitivities of 0.746 and 0.761 mV/(μg/mL), respectively. The limit of detection (LOD) was also very low at 0.419 and 0.428 μg/mL. These findings show that Fe_3O_4/chitosan nanocomposites integrated GMR chip-based sensors can be a dependable instrument for detecting a variety of biomolecules such as Bovine serum albumin (BSA).

Informasi Artikel

Proses artikel:
Diterima 13 Oktober 2024
Diterima dan direvisi dari 5 November 2024
Accepted 7 November 2024

Kata kunci: *Giant Magnetoresistance, Fe_3O_4/kitosan, Label magnetik, kopresipitasi, sensor*

Abstrak

Penelitian ini menjelaskan bagaimana komposisi fasa mempengaruhi kemampuan sensor berbasis chip giant magnetoresistance (GMR) untuk mendeteksi label magnetik yang terbuat dari Fe_3O_4 dan Fe_3O_4/kitosan yang disintesis dengan metode kopresipitasi. Analisis difraksi sinar-X (XRD) mengungkapkan bahwa nanopartikel yang disintesis merupakan campuran fase magnetit dan maghemit. Puncak difraksi yang paling kuat pada 2θ = 35,6° (311) mengkonfirmasi keberadaan fase magnetit. Penambahan kitosan secara signifikan meningkatkan proporsi fase maghemite dari 10% menjadi 25%, dengan munculnya puncak tambahan pada 2θ = 33° (221). Modifikasi nanopartikel Fe_3O_4 menjadi nanokomposit Fe_3O_4/kitosan mengakibatkan perubahan sensitivitas sensor. Sensor GMR berhasil mendeteksi label magnetik Fe_3O_4 dan Fe_3O_4/kitosan dalam waktu 30 detik dengan sensitivitas tinggi masing-masing 0,746 dan 0,761 mV/(μg/mL). Batas deteksi (LOD) juga sangat rendah yaitu 0,419 dan 0,428 (μg/mL). Temuan ini menunjukkan bahwa sensor berbasis chip GMR nanokomposit Fe3O4/kitosan terintegrasi dapat menjadi instrumen yang dapat diandalkan untuk mendeteksi berbagai biomolekul.

* Corresponding author.
E-mail address: *yuvita.oktarisa@untirta.ac.id, *ganesha.antarnusa@untirta.ac.id

1. Introduction

Giant magnetoresistance (GMR) sensors, since their introduction in 1988, have transformed the field of data storage technology by their widespread usage of magnetoresistive random-access memory (MRAM) and hard disc drives (HDD). The high sensitivity to magnetic field changes, which is a key characteristic of GMR sensors, has opened up new opportunities in the field of biosensing. In 1998, researchers began to explore the potential of GMR sensors as biomolecule detection devices (Baselt et al., 1998). The intrinsic advantages of GMR sensors such as portability, relatively low production cost, high sensitivity, and real-time readout capability electronically make them a promising platform in biosensor development (Ardiyanti et al., 2023). GMR sensors have high electronic compatibility, making integration with other electronic devices easier. In addition, the instrumentation techniques required are relatively simple, and their flexible design enables fabrication on a micro (chip) scale (Giouroudi & Hristoforou, 2018). The performance stability of GMR-based biosensors that are not affected by pH and temperature fluctuations makes these devices very promising for biomolecule detection applications (Cao et al., 2020).

Detection of biomolecules with GMR sensors requires an indirect approach through magnetic labelling. This is due to the inability of GMR sensors to directly detect molecules that are not magnetic. Magnetic nanoparticles (NPMs) act as magnetic markers that enable the detection of target biomolecules. The most commonly used magnetic labels are iron oxide-based ferromagnetic materials, such as Fe_3O_4, $CoFe_2O_4$, $NiFe_2O_4$, $MnFe_2O_4$, and $NiZnFe_2O_4$ (Antarnusa, Jayanti, et al., 2022; Hutchins et al., 2007; Panda et al., 2014; Xu et al., 2016; Zhang et al., 2018). Fe_3O_4 nanoparticles, with high saturation magnetization, offer great potential as magnetic labels in various applications, thanks to their ability to generate strong magnetic fields and responsiveness to external fields (Wu et al., 2019). The synthesis of Fe_3O_4 magnetic nanoparticles is commonly carried out through hydrothermal, sol-gel, and chemical co-precipitation methods (Ferreira et al., 2020). Among the three methods, chemical co-precipitation is often the first choice because the process is simple, fast, does not require extreme conditions such as high temperatures, and allows better control of particle size (Ganapathe et al., 2020). However, since Fe_3O_4 produces high magnetic properties, these nanoparticles are prone to agglomeration and easily oxidized (Ganapathe et al., 2020; Majidi et al., 2014). Therefore, in order to obtain physically stable magnetic labels for biosensors, Fe_3O_4 nanoparticles should be composited with other materials that have certain functional properties (Dizaji et al., 2016).

Chitosan materials have the ability to prevent agglomeration (Koesnarpadi et al., 2020) and have promising potential to be applied in the development of GMR biosensors (Garcia et al., 2024). As a stabilizing agent for Fe_3O_4 nanoparticles, chitosan offers a number of advantages that synthetic polymers do not. Its natural, environmentally friendly, and harmless to the body properties make it a very attractive option in the development of various biomedical applications. The addition of chitosan on the surface of Fe_3O_4 nanoparticles (Fe_3O_4/chitosan) can improve chemical stability, prevent aggregation, protect the surface of nanoparticles from oxidation damage, and provide additional functions thanks to the presence of specific functional groups on the chitosan molecule (Karaca et al., 2015).

GMR sensor chips are crucial sensing components in biosensor systems that utilize magnetic labels. Various technologies continue to be developed so that they can be applied in chip form, including GMR sensors. Currently, several chip manufacturers have produced GMR chips that are commercially marketed, such as Sensitec GmbH (Germany) and Nonvolatile Electronics (NVE) Corp. (United States). Several studies have developed biosensors based on GF708, a GMR chip produced by Sensitec. Guan et al. (Guan et al., 2019), Zhang et al. (Zhang et al., 2019), and Yuan et al. (Yuan et al., 2021) have reported the detection of NPMs using GF708. This characteristic makes it highly suitable for use in various magnetic field detection applications (Baselt et al., 1998). Several previous studies have also reported the utilisation of Fe_3O_4 material as a sensor component, as described in the study by (Antarnusa et al., 2022; Zhang et al., 2019) . This shows the significant potential of Fe_3O_4 for detection applications in magnetic fields. With reference to these previous studies, this research seeks to fill the research gap with a new approach of Fe3O4/Chitosan using GF708 as a sensor to detect NPM more effectively.

This research aims to develop the use of GMR chip sensors in the field of biological detection by integrating Fe_3O_4/chitosan magnetic labels. To acquire an accurate signal, the detecting system is fitted with a differential amplifier and an Arduino microcontroller. To guarantee the stability and functionality of the magnetic label, a comprehensive characterization of the phase composition and size of the Fe_3O_4/chitosan nanocomposite was carried out. The evaluation of the GMR sensor's performance was conducted using several characteristics, including linearity, sensitivity, repeatability, and relative standard deviation (RSD).

2. Research Methods

2.1. Synthesis of Fe_3O_4/chitosan nanocomposites

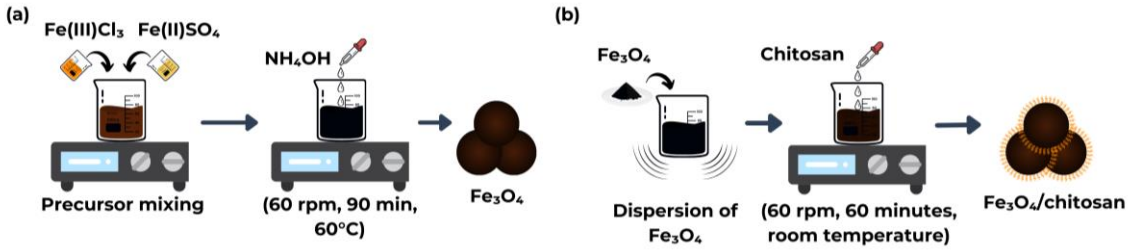

Figure 1. Schematic illustration of Fe_3O_4/chitosan nanocomposite synthesis. (a) Fe_3O_4 synthesis process using co-precipitation method, (b) preparation of Fe_3O_4/chitosan nanocomposite.

2.1.1. Synthesis of Fe_3O_4

The Fe_3O_4 nanoparticles were synthesized using a simple co-precipitation method, as illustrated in Figure 1(a) and detailed in a previous research (Cuana et al., 2022). 7.5 mL of distilled water were used to dissolve 4.054 g of

$FeCl_3.6H_2O$ and 2.086 g of $FeSO_4.7H_2O$, which were then agitated for 15 minutes. Then the two solutions were mixed together and stirred using a magnetic stirrer at 60°C for 15 minutes until the solution was homogeneous. Subsequently, 40 mL of a 10% NH_4OH solution was added dropwise using a drop pipette, and the mixture was stirred at 600 rpm at 60°C for 90 minutes. The Fe_3O_4 solution was precipitated and washed with distilled water 7 times until the pH was neutral. The precipitation process was assisted by a magnetic table so that the particles could be easily separated from the solvent. Next, the Fe_3O_4 precipitate was dried using a furnace at 100°C for 2 hours and then crushed into Fe_3O_4 powder.

2.1.2. Synthesis of Fe_3O_4/chitosan

After obtaining Fe_3O_4 powder via the co-precipitation method, the next step was to prepare Fe_3O_4/chitosan nanoparticles. Using ultrasonication, 0.8 g of Fe_3O_4 nanoparticles were distributed throughout 25 ml of distilled water. For 30 minutes, 0.2 g of chitosan was simultaneously dissolved in 25 ml of a 2% acetic acid (CH_3COOH) solution. The Fe_3O_4 nanoparticles were then combined with the chitosan solution. The chitosan solution was thoroughly mixed with the Fe_3O_4 nanoparticles for an hour at a steady speed of 600 rpm. The excess polymer was then removed from the Fe_3O_4/chitosan nanoparticles by precipitating them with a magnet and washing them seven times in distilled water. The precipitate was then dried in a furnace for two hours at 80°C to produce Fe_3O_4/chitosan nanoparticles. In Figure 1(b), the procedure is depicted.

2.2. Characterization of Fe_3O_4/chitosan

XRD analysis using a Shimadzu Bruker D8 Advance diffractometer with Cu-Kα radiation is a commonly used method to characterize the crystal structure of nanomaterials.

2.3. Sensor configuration and design

The experimental scheme used for this study utilizes a constant current of 10 mA flowing through the power supply to generate a uniform magnetic field on the Helmholtz coil, which then affects the sensitivity of the GF708 GMR sensor. The magnetic label was dispersed in ethanol using sonication for 15 minutes before being applied to the GMR sensor surface. 2 µL of magnetic label was dropped onto the GMR chip. After the ethanol evaporated, only the sample remained on the sensor surface. A magnetic field that remains unchanged over time (H_B) was used after the solvent evaporated, and the output voltage (V_{out}) of each Fe_3O_4 and Fe_3O_4/chitosan label type was recorded for 30 seconds. For sensor performance evaluation, the test used five concentrations: 0.1, 1, 10 and 100 μg/mL. The signal derived from the magnetic label is obtained by output voltage signal (V_{out}) with the background signal ($V_{0\text{-}chip}$) obtained from measurements in the absence of the magnetic label, as mentioned in Eq. (1).

$$Signal = \left|V_{out} - V_{0-Chip}\right| \tag{1}$$

3. Results and Discussions

3.1. XRD analysis

The XRD peaks of Fe_3O_4 and Fe_3O_4/chitosan nanocomposites are depicted in Figure 2. According to the XRD pattern of Fe_3O_4 NPs, the diffraction peaks of Fe_3O_4/chitosan correspond to the crystal planes of (220), (311), (400), (422), (511), and (440). According to the Cif. (COD. 1010369), these peaks show a cubic inverted spinel structure. Part of the Fe_3O_4 NPs may be oxygen-susceptible during the surface adjustment process, which causes the oxidation reaction to shift the phase to maghemite (γ- Fe_2O_3). This is in line with previous research findings by Garcia et al (Garcia et al., 2024).

$$2Fe_3O_4 + 1/2O_2 \rightarrow 3\gamma - Fe_2O_3$$

However, the diffraction pattern of Fe_3O_4 nanoparticles with chitosan addition showed the formation of another phase, maghemite (γ- Fe_2O_3, Cif (COD. 9006316)) which was detected at an angle of 2θ: 33.1° (221). This results from oxidation that occurs when nanoparticles are modified and dried.

The modification process increases the interaction between Fe_3O_4 and chitosan. The protonated chitosan binds electrostatically with Fe_3O_4, forming larger crystals (Andrade et al., 2017). The crystallite sizes of Fe_3O_4 and Fe_3O_4/chitosan were calculated using the Debye-Scherrer equation (see Equation (2)). Crystallite size analysis showed an increase from 10.7 nm in Fe_3O_4 to 10.9 nm in Fe_3O_4/chitosan nanocomposite. The addition of chitosan to the nanocomposite is the cause of this rise in crystallite size value. The addition of a new layer caused by the surface modification process of Fe_3O_4 nanoparticles led to an increase in crystallite size. When compared to normal Fe_3O_4, the diffraction intensity of Fe_3O_4/chitosan nanoparticles is lower. This drop in intensity shows that amorphous chitosan has been effectively coated on the surface of Fe3O4 nanoparticles. (Pourmortazavi et al., 2019; Zadvarzi et al., 2021). The lattice parameter values obtained for Fe_3O_4 and Fe_3O_4/chitosan are consistent at 8.16 Å.

$$D = \frac{k\lambda}{\beta \cos\theta} \tag{2}$$

The wavelength of incoming Cu-Kα radiation (λ = 1.5406 Å), the full width at half maximum (FWHM) (β), the crystallite size (D nm), and the Scherrer constant (k = 0.94) are all related to the Bragg diffraction angle (θ).

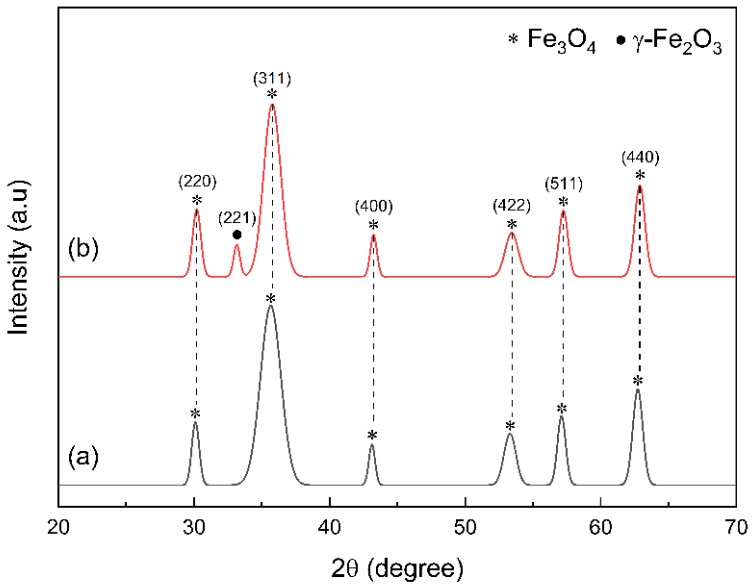

Figure 2. XRD patterns of (a) Fe_3O_4 and (b) Fe_3O_4/chitosan nanocomposites with a mass ratio of 4:1.

3.2. The ability of the sensor to detect magnetic labels

Research on key parameters such as sensitivity, linearity, and limit of detection (LOD) is crucial in GMR chip-based sensor systems. The performance of GMR sensors used to detect magnetic labels was assessed in this work using Fe_3O_4 and Fe_3O_4/chitosan nanocomposites with a mass ratio of 4:1. Figure 3 presents the results of the GMR sensor's ability to identify these labels. For each of the four magnetic label concentrations—0.1, 1, 10, and 100 µg/mL—signal measurements were conducted three times. The sensor-maintained stability for 30 seconds. Additionally, the system operates rapidly, offering quick detection times. The signal intensity also increases with higher magnetic label concentrations, confirming that Fe_3O_4 and Fe_3O_4/chitosan nanocomposites can effectively produce stray fields below 1.7 Oe of bias magnetic field (H_B), which the GMR sensor can identify with accuracy. As a result, due to its minimal magnetic field outside requirement and fast detection time, the GMR sensor shows strong potential for development as an affordable, energy-efficient, and user-friendly biosensor (Antarnusa et al., 2018).

The presence of maghemite (γ- Fe_2O_3) in the sample can have a significant impact on the performance of the GMR sensor. Maghemite has different magnetic properties from magnetite (Fe_3O_4). This difference in magnetic properties can affect the interaction between magnetic particles and the magnetic layer on the GMR sensor. If the proportion of maghemite is large enough, it may cause a decrease in sensor sensitivity, an increase in noise, or a change in the magnetoresistance curve. The results of this study are in line with Antarnusa's findings showing that crystal size has a significant influence on GMR sensor performance (Antarnusa et al., 2022). An increase in crystal size generally correlates with an increase in material coercivity, which can reduce the sensitivity of the sensor. This is due to the reduced magnetic domains that can be easily reversed by an external magnetic field.

The linear correlation between the concentration of magnetic labels and the output signal of the sensor is depicted in Figure 4(a). The response of the GMR sensor to different magnetic label concentrations shows high linearity, as demonstrated by the value of the coefficient of determination (R^2). For Fe_3O_4 nanoparticles, the sensor exhibits a sensitivity of 0.746 mV/(µg/mL) and a detection limit (LOD) of 0.419 µg/mL. In contrast, the Fe_3O_4/chitosan nanocomposite shows reduced sensitivity, with a value of 0.761 µg/mL and an LOD of 0.428 µg/mL, as summarized in Table 1.

The Fe_3O_4 nanoparticles only produce a weak stray field at very low concentrations. Conversely, upon an increase in magnetic label concentration, more Fe_3O_4 nanoparticles accumulate on the sensor surface, proving that the magnetic labels' effects on the stray field intensity can be detected by the GF708 GMR sensor. According to (Zhang et al., 2019), the sensitivity of the sensor is affected by the strength of the stray field, which is influenced by the size of the magnetic nanoparticles. As a result, Fe_3O_4 nanoparticles without chitosan exhibited the highest sensitivity. Conversely, Figure 4(b) presents the Relative Standard Deviation (RSD) values produced by Fe_3O_4/chitosan, with Equation 3 being used to compute the voltage signal's RSD.

$$RSD = \frac{\sqrt{\frac{\sum_{i=1}^{n}\left(V_x - \bar{V}\right)^2}{n-1}}}{\bar{V}\times 100}\% \quad (3)$$

Prayoga GA, Oktarisa Y, Antarnusa G, Fitriani NS, Aryani RM, Suherman A, and Guntara Y, 2024, The Effect of Chitosan Addition on Phase Composition and Detection Sensitivity of Fe_3O_4/Chitosan Magnetic Label Nanoparticles Based on Giant Magnetoresistance Sensor, *Journal of Energy, Material, and Instrumentation Technology* Vol. 5 No. 4, 2024

Analysis of the variation in output voltage (V_x) showed good detection repeatability RSD of 0.19 – 0.12 % for Fe_3O_4 and RSD of 0.16 – 0.13 % for Fe_3O_4/chitosan, indicating reliable sensor performance. The correlation between the decrease in Relative Standard Deviation (RSD) and the increase in magnetic label concentration, which is consistent with the Horwitz Trumpet model, shows an increase in precision as the number of labels increases (Wibowo et al., 2022). Modification of Fe_3O_4 nanoparticles into Fe_3O_4/chitosan nanocomposites influenced e sensor's sensitivity and slope, although not significantly. Fe_3O_4/chitosan nanocomposite shows promise as a magnetic label for use in giant magnetoresistance (GMR) sensor systems, according to the study's findings.

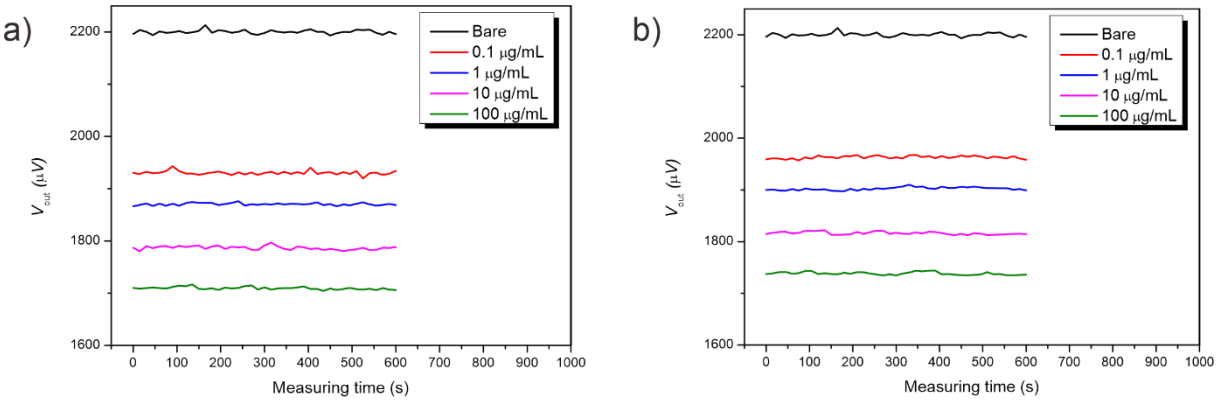

Figure 3. Signal measurements: (a) Fe_3O_4, and (b) Fe_3O_4/chitosan nanocomposite with a mass ratio of 4:1.

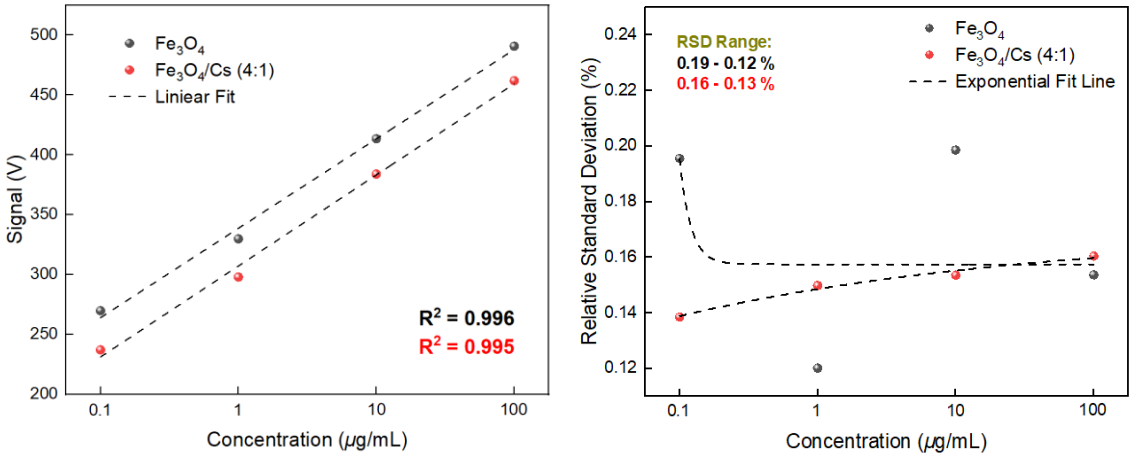

Figure 4. (a) The relationship between the sensor signal and the magnetic label concentration, and (b) the relative deviation of the repeated signal measurements.

Table 1 Sensitivity, LOD, and R^2 of Fe_3O_4 and Fe_3O_4/chitosan nanocomposites

Nanomaterial	Sensitivity (mV/(μg/mL))	LOD (μg/mL)	R^2
Fe_3O_4	0.746	0.419	0.996
Fe_3O_4/chitosan	0.761	0.428	0.995

The magnetic label detection mechanism on the GF708 GMR chip sensor, as illustrated in Figure 5, involves three main stages. Firstly, 0.1 μL of magnetic label dispersion in ethanol is dripped on the surface of the sensor element. After the ethanol evaporates, a constant bias magnetic field (H_B) is applied parallel to the easy axis of magnetization of the sensor (see Figure 5(a)). The use of in-plane DC mode allows higher tolerance to misalignment of the external magnetic field, making it suitable for portable sensor applications. Figure 5(b) illustrates the condition where there is no external bias magnetic field (H_B). In this condition, the resistance of the sensor reaches its maximum value due to significant scattering of electrons resulting from the antiparallel arrangement of the fixed layer's and the free layer's magnetic moments. The application of a bias field will reverse the magnetic moment of the free layer to align with that of the fixated layer, thus lowering the resistance. The difference in the sensor output voltage is a direct consequence of this change in resistance.

The bias field creates an overlapping magnetic field of the magnetic label in addition to altering the magnetization of the sensor's top layer. The direction of these overlapping fields is opposite to the direction of the bias field in the in-plane DC configuration, so the effectiveness of the total magnetic field acting on the sensor element

is reduced. These overlapping fields cause enhanced electron scattering, which raises the resistance of the sensor when magnetic labels are applied to the chip's surface. An increase in magnetic label concentration correlates with an increase in the overlap field and sensor resistance, indicating the presence of more Fe_3O_4 nanoparticles adsorbed on the chip surface. Further analysis in the bias field range of 0 to 1.7 Oe shows that the maximum resistance (R_{max}) is larger than the resistance in the condition with bias field (R_c, R_b, R_a).

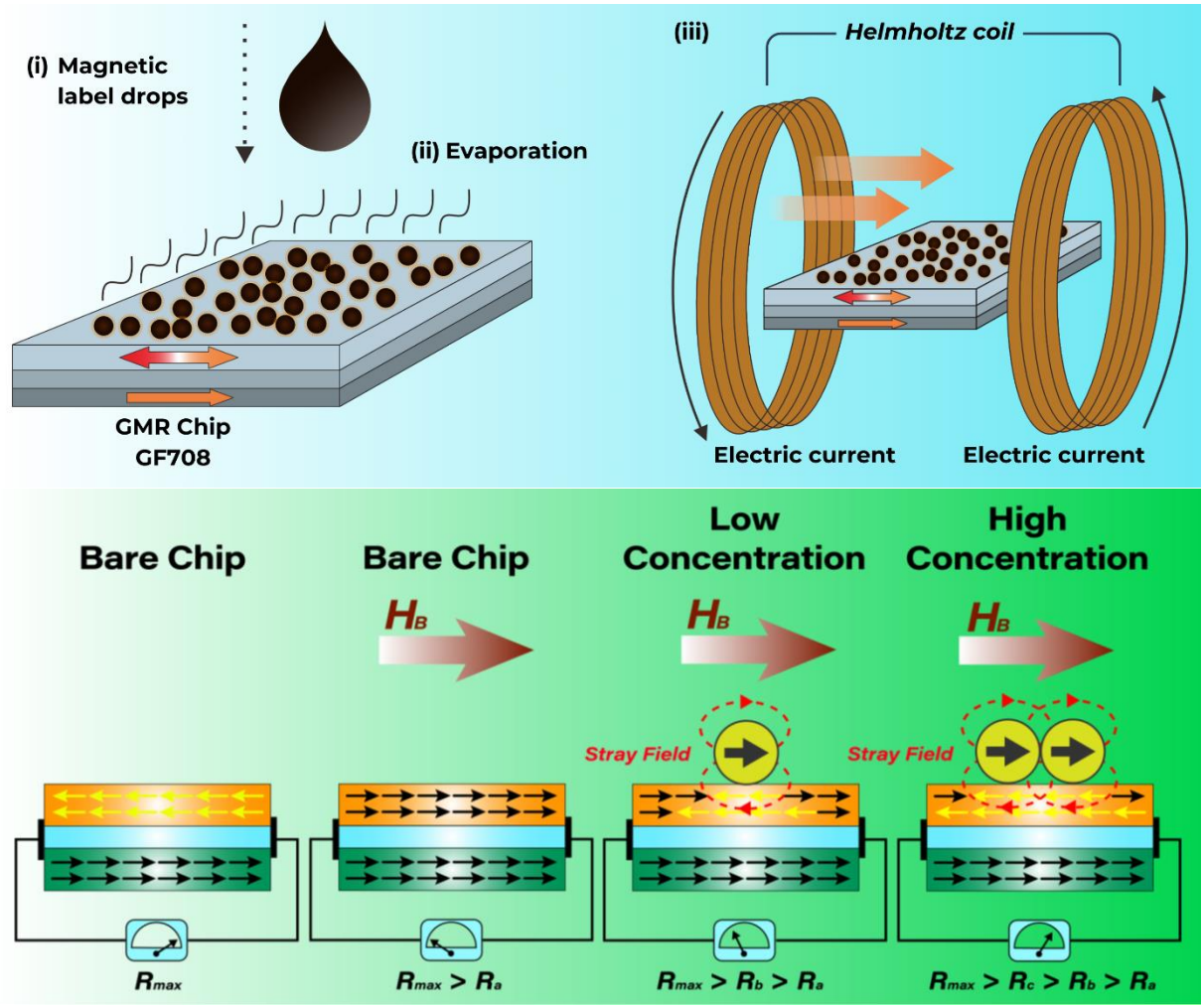

Figure 5. An illustration of the GF708 GMR chip's ability to detect magnetic labels (a) and how the sensor's resistance changes depending on the magnetic label's interference field (b)

The GF708 GMR sensor works by utilizing the change in electrical resistance due to the presence of a magnetic field. When a magnetic label containing Fe_3O_4 particles is placed on top of the sensor, these particles will create a local magnetic field that is opposite in direction to the bias field that has been applied. The presence of this opposing magnetic field will disturb the magnetic equilibrium in the thin layer inside the GMR sensor, causing an increase in electrical resistance. The more magnetic labels attached to the sensor surface, the greater the increase in resistance. Thus, this change in resistance can be used as a signal to detect the presence and concentration of magnetic labels, which in turn can be used to measure the concentration of a substance in a sample.

4. Conclusions

Real-time detection of Fe_3O_4 nanoparticles has been carried out using the GF708 GMR sensor transducer combined with Fe_3O_4/chitosan nanocomposite as a magnetics label. This GMR sensor shows excellent performance in monitoring changes in the output voltage of the magnetic label, which is evident from the consistent and stable measurement results. The sensor easily detects changes in output voltage caused by variations in the strength of the magnetic field generated by the label. The GMR sensor showed good sensitivity to the magnetic label concentration, with a sensitivity of 0.746 mV/(μg/mL) for Fe_3O_4 and 0.761 mV/(μg/mL) for Fe_3O_4/chitosan, although the Fe_3O_4/chitosan nanocomposite had a lower sensitivity. The sensor showed good stability and linearity, with a limit of detection (LOD) of 0.419 μg/mL for Fe_3O_4 and 0.428 μg/mL for Fe_3O_4/chitosan. Based on these findings, a quick and useful biosensor system was created by fusing the Fe_3O_4/chitosan magnetic label with the GMR chip-based sensor.

5. Acknowledgement

This work was funded by Universitas Sultan Ageng Tirtayasa through the 'Penelitian Dosen Madya, DIPA 2024' research scheme. The author would like to thank Universitas Sultan Ageng Tirtayasa for facilitating this research.

6. Bibliography

Andrade, A. B., Ferreira, N. S., & Valerio, M. E. G. (2017). Particle size effects on structural and optical properties of BaF2 nanoparticles. *RSC Advances*, *7*(43), 26839–26848. https://doi.org/10.1039/c7ra01582h

Antarnusa, G., Elda Swastika, P., & Suharyadi, E. (2018). Wheatstone bridge-giant magnetoresistance (GMR) sensors based on Co/Cu multilayers for bio-detection applications. *Journal of Physics: Conference Series*, *1011*(1), 8–13. https://doi.org/10.1088/1742-6596/1011/1/012061

Antarnusa, G., Esmawan, A., Dwi Jayanti, P., Rizki Fitriani, S., Suherman, A., Kinarya Palupi, E., Umam, R., & Ardimas. (2022). Synthesis of Fe3O4 at different reaction temperatures and investigation of its magnetic properties on giant magnetoresistance (GMR) sensors for bio-detection applications. *Journal of Magnetism and Magnetic Materials*, *563*(September), 169903. https://doi.org/10.1016/j.jmmm.2022.169903

Antarnusa, G., Jayanti, P. D., Denny, Y. R., & Suherman, A. (2022). Utilization of co-precipitation method on synthesis of Fe3O4 / PEG with different concentrations of PEG for biosensor applications Materialia Utilization of co-precipitation method on synthesis of Fe 3 O 4 / PEG with different concentrations of PEG for bi. *Materialia*, *25*(March 2024), 101525. https://doi.org/10.1016/j.mtla.2022.101525

Ardiyanti, H., Mabarroh, N., Wibowo, N. A., Istiqomah, N. I., Tumbelaka, R. M., Ulil Absor, M. A., & Suharyadi, E. (2023). New design of a commercial chip-based GMR sensor with magnetite nanoparticles for biosensing applications. *Journal of Science: Advanced Materials and Devices*, *8*(2), 100556. https://doi.org/10.1016/j.jsamd.2023.100556

Baselt, D. R., Lee, G. U., Natesan, M., Metzger, S. W., Sheehan, P. E., & Colton, R. J. (1998). A biosensor based on magnetoresistance technology1This paper was awarded the Biosensors & Bioelectronics Award for the most original contribution to the Congress.1. *Biosensors and Bioelectronics*, *13*(7–8), 731–739. http://linkinghub.elsevier.com/retrieve/pii/S0956566398000372

Cao, B., Wang, K., Xu, H., Qin, Q., Yang, J., Zheng, W., Jin, Q., & Cui, D. (2020). Development of magnetic sensor technologies for point-of-care testing: Fundamentals, methodologies and applications. *Sensors and Actuators, A: Physical*, *312*, 112130. https://doi.org/10.1016/j.sna.2020.112130

Cuana, R., Panre, A. M., Istiqomah, N. I., Tumbelaka, R. M., Sunaryono, Wicaksono, S. T., & Suharyadi, E. (2022). Green Synthesis of Fe 3 O 4 /Chitosan Nanoparticles Utilizing Moringa Oleifera Extracts and Their Surface Plasmon Resonance Properties . *ECS Journal of Solid State Science and Technology*, *11*(8), 083015. https://doi.org/10.1149/2162-8777/ac8b36

Dizaji, A. N., Yilmaz, M., & Piskin, E. (2016). Silver or gold deposition onto magnetite nanoparticles by using plant extracts as reducing and stabilizing agents. *Artificial Cells, Nanomedicine and Biotechnology*, *44*(4), 1109–1115. https://doi.org/10.3109/21691401.2015.1019672

Ferreira, M., Sousa, J., Pais, A., & Vitorino, C. (2020). The role of magnetic nanoparticles in cancer nanotheranostics. *Materials*, *13*(2), 266.

Ganapathe, L. S., Mohamed, M. A., & Yunus, R. M. (2020). Magnetite (Fe 3 O 4) Nanoparticles in Biomedical Application : From Synthesis to Surface Functionalisation. *Magnetochemistry*, *6*(4), 68.

Garcia, S., Mabarroh, N., Cuana, R., Ardiyanti, H., Istiqomah, N. I., & Suharyadi, E. (2024). Detection of Green-Synthesized Fe_3O_4/ Chitosan Using Spin Valve GMR Sensor with Wheatstone Bridge Circuit. *Materials Science Forum*, *1114*(March), 9–14. https://doi.org/10.4028/p-7ulydw

Giouroudi, I., & Hristoforou, E. (2018). Perspective: Magnetoresistive sensors for biomedicine. *Journal of Applied Physics*, *124 (3)*. https://doi.org/10.1063/1.5027035

Guan, M., Mu, X., Zhang, H., Zhang, Y., Xu, J., Li, Q., Wang, X., Cao, D., & Li, S. (2019). Spindle-like Fe3O4 nanoparticles for improving sensitivity and repeatability of giant magnetoresistance biosensors. *Journal of Applied Physics*, *126*(6). https://doi.org/10.1063/1.5096345

Hutchins, B. M., Platt, M., Hancock, W. O., & Williams, M. E. (2007). Directing transport of CoFe2O4-functionalized microtubules with magnetic fields. *Small*, *3*(1), 126–131. https://doi.org/10.1002/smll.200600410

Karaca, E., Şatir, M., Kazan, S., Açikgöz, M., Öztürk, E., Gürdaı, G., & Ulutaş, D. (2015). Synthesis, characterization and magnetic properties of Fe3O4 doped chitosan polymer. *Journal of Magnetism and Magnetic Materials*, *373*, 53–59. https://doi.org/10.1016/j.jmmm.2014.02.016

Koesnarpadi, S., Astuti, W., & Lianasari, I. Y. (2020). Nanoparticles Fe3O4 modified chitosan and its antibacterial applications. *AIP Conference Proceedings*, *2237*(June), 10–15. https://doi.org/10.1063/5.0005693

Majidi, S., Sehrig, F. Z., Farkhani, S. M., & Goloujeh, M. S. (2014). Current methods for synthesis of magnetic nanoparticles Current methods for synthesis of magnetic nanoparticles. *Artificial Cells, Nanomedicine, and Biotechnology*, *44 (2)*(December 2017). https://doi.org/10.3109/21691401.2014.982802

Panda, J., Saha, S. N., & Nath, T. K. (2014). Room temperature giant positive junction magnetoresistance of NiFe 2O4/n-Si heterojunction for spintronics application. *Physica B: Condensed Matter*, *448*, 184–187. https://doi.org/10.1016/j.physb.2014.04.002

Pourmortazavi, S. M., Sahebi, H., Zandavar, H., & Mirsadeghi, S. (2019). Fabrication of Fe3O4 nanoparticles coated by extracted shrimp peels chitosan as sustainable adsorbents for removal of chromium contaminates from wastewater: The design of experiment. *Composites Part B: Engineering*, *175*(July), 107130. https://doi.org/10.1016/j.compositesb.2019.107130

Wibowo, N. A., Sabarman, H., & Suharyadi, E. (2022). A New Platform of Iron Oxide-Based Nanoparticles Assay Using GMR Chip-Based Sensor With Microcontroller. *IEEE Sensors Journal*, *22*(21), 20093–20101. https://doi.org/10.1109/JSEN.2022.3207213

Wu, K., Su, D., Saha, R., Liu, J., & Wang, J.-P. (2019). Investigating the Effect of Magnetic Dipole-Dipole Interaction on Magnetic Particle Spectroscopy (MPS): Implications for Magnetic Nanoparticle- based Bioassays and Magnetic Particle Imaging (MPI). *Journal of Physics D: Applied Physics*, *52 (33)*, 0–16.

Xu, J., Li, Q., Zong, W., Zhang, Y., & Li, S. (2016). Ultra-wide detectable concentration range of GMR biosensors using Fe3O4 microspheres. *Journal of Magnetism and Magnetic Materials*, *417*, 25–29. https://doi.org/10.1016/j.jmmm.2016.05.059

Yuan, S., Du, Y., & Pong, P. W. T. (2021). A Linear Slope Analyzing Strategy of GMR Sensor Transfer Curve for Static Detection of Magnetic Nanoparticles. *IEEE Sensors Journal*, *21*(21), 23934–23942. https://doi.org/10.1109/JSEN.2021.3110609

Zadvarzi, S. B., Khavarpour, M., Vahdat, S. M., Baghbanian, S. M., & Rad, A. S. (2021). Synthesis of Fe3O4@chitosan@ZIF-8 towards removal of malachite green from aqueous solution: Theoretical and experimental studies. *International Journal of Biological Macromolecules*, *168*, 428–441. https://doi.org/10.1016/j.ijbiomac.2020.12.067

Zhang, Y., Xu, J., Cao, D., Li, Q., Zhao, G., Sun, N. X., & Li, S. (2018). Journal of Magnetism and Magnetic Materials The influence of bias magnetization of nanoparticles on GMR sensor signal and sensitivity for the ultra-low concentration detection. *Journal of Magnetism and Magnetic Materials*, *453*, 132–136. https://doi.org/10.1016/j.jmmm.2018.01.010

Zhang, Y., Xu, J., Li, Q., Cao, D., & Li, S. (2019). The effect of the particle size and magnetic moment of the Fe 3 O 4 superparamagnetic beads on the sensitivity of biodetection. *AIP Advances*, *9*(1). https://doi.org/10.1063/1.5050034